

High power pulsed magnetron sputtering: A method to increase deposition rate

Priya Raman, Ivan A. Shchelkanov, Jake McLain, and David N Ruzic

Citation: *Journal of Vacuum Science & Technology A* **33**, 031304 (2015); doi: 10.1116/1.4916108

View online: <http://dx.doi.org/10.1116/1.4916108>

View Table of Contents: <http://scitation.aip.org/content/avs/journal/jvsta/33/3?ver=pdfcov>

Published by the AVS: Science & Technology of Materials, Interfaces, and Processing

Articles you may be interested in

Method to control deposition rate instabilities—High power impulse magnetron sputtering deposition of TiO₂
J. Vac. Sci. Technol. A **33**, 021514 (2015); 10.1116/1.4905737

Modified high power impulse magnetron sputtering process for increased deposition rate of titanium
J. Vac. Sci. Technol. A **31**, 060604 (2013); 10.1116/1.4819296

Effects of the magnetic field strength on the modulated pulsed power magnetron sputtering of metallic films
J. Vac. Sci. Technol. A **29**, 061301 (2011); 10.1116/1.3645612

On the deposition rate in a high power pulsed magnetron sputtering discharge
Appl. Phys. Lett. **89**, 154104 (2006); 10.1063/1.2362575

High-rate deposition of MgO by reactive ac pulsed magnetron sputtering in the transition mode
J. Vac. Sci. Technol. A **24**, 106 (2006); 10.1116/1.2138717

ADVERTISEMENT

Instruments for advanced science

Gas Analysis



- dynamic measurement of reaction gas streams
- catalysis and thermal analysis
- molecular beam studies
- dissolved species probes
- fermentation, environmental and ecological studies

Surface Science




- UHV TPD
- SIMS
- end point detection in ion beam etch
- elemental imaging - surface mapping

Plasma Diagnostics



- plasma source characterization
- etch and deposition process reaction kinetic studies
- analysis of neutral and radical species

Vacuum Analysis



- partial pressure measurement and control of process gases
- reactive sputter process control
- vacuum diagnostics
- vacuum coating process monitoring

contact Hiden Analytical for further details



info@hideninc.com
www.HidenAnalytical.com
 CLICK to view our product catalogue 

High power pulsed magnetron sputtering: A method to increase deposition rate

Priya Raman^{a)}

Center for Plasma Material Interactions, University of Illinois, Urbana, Illinois 61801

Ivan A. Shchelkanov

Center for Plasma Material Interactions, University of Illinois, Urbana, Illinois 61801 and National Nuclear Research University MEPhI (Moscow Engineering Physics Institute), Moscow 115409, Russia

Jake McLain and David N Ruzic

Center for Plasma Material Interactions, University of Illinois, Urbana, Illinois 61801

(Received 10 October 2014; accepted 12 March 2015; published 25 March 2015)

High power pulsed magnetron sputtering (HPPMS) is a state-of-the-art physical vapor deposition technique with several industrial applications. One of the main disadvantages of this process is its low deposition rate. In this work, the authors report a new magnetic field configuration, which produces deposition rates twice that of conventional magnetron's dipole magnetic field configuration. Three different magnet pack configurations are discussed in this paper, and an optimized magnet pack configuration for HPPMS that leads to a higher deposition rate and nearly full-face target erosion is presented. The discussed magnetic field produced by a specially designed magnet assembly is of the same size as the conventional magnet assembly and requires no external fields. Comparison of deposition rates with different power supplies and the electron trapping efficiency in complex magnetic field arrangements are discussed. © 2015 American Vacuum Society. [<http://dx.doi.org/10.1116/1.4916108>]

I. INTRODUCTION

Physical vapor deposition (PVD) techniques dominate the thin film coating industry and the need for high quality coatings is continuing to increase. Magnetron sputtering is one of the most widely used PVD techniques. The magnetic field configuration above the target allows one to obtain a higher and stable discharge current at lower pressures than in a normal glow discharge. The cylindrical symmetry of the conventional planar magnetron gives rise to an arch shaped magnetic field configuration above the target surface. In this paper, the arch shaped magnetic field configuration will be referred to as “conventional” design. This design was developed 30 years ago and the direct current (DC) charges in it have been studied since then.¹ Ionized PVD (iPVD) is a class of PVD technique in which >50% of the deposition flux may be ionized.² Since ion energy and direction is easy to control, iPVD techniques are used in a wide variety of applications like the formation of diffusion barriers and seed layers on the side and bottom of high aspect ratio trenches and vias in the microelectronics industry, enhancing substrate pretreatment to improve adhesion of hard coatings, depositing wear and corrosion resistant coatings, etc.³

High power pulsed magnetron sputtering (HPPMS) is a type of iPVD technique where short high-peak-power (up to 3 kW/cm²) pulses are applied to the magnetron sputter target at low duty cycles (0.5%–10%). HPPMS discharges can be operated in the conventional magnet pack. This results in plasma electron densities as high as 10¹⁹ m⁻³ above the target surface during the short high-power pulses.^{4,5} These high electron densities near the target enhance ionization of

sputtered materials.⁶ The now-ionized sputtered material is accelerated back to the target resulting in an increase in the sputtering rate by having the discharge go into a self-sputtering mode.⁷ Some sputtered ions escape and provide superior deposited film quality on the substrate. Electron trapping efficiency and magnetic field influence on the plasma potential distribution will be discussed later in the paper. The films that are grown using HPPMS technique are denser, smoother, and have better adhesion to the substrate than the films deposited by direct current magnetron sputtering (dcMS).⁸

Mozgrin *et al.*,⁹ first reported on a high power pulsed magnetron discharge with pulse deposition rates no less than 80 μm/min at a distance of 120 mm from the cathode with 2 kJ pulse energy. Following this, a highly cited publication by Kouznetsov *et al.*,⁶ reported that the deposition rate of HPPMS was 80% lower than dcMS with high frequency low energy pulses. Since then, deposition rates for different target materials were compared in dcMS and high power impulse magnetron sputtering (HiPIMS) discharges for the same average power by Samuelsson *et al.*¹⁰ The HiPIMS deposition rates were consistently lower for all the target materials. In the case of aluminum targets, the deposition rate in HiPIMS was only 50% of dcMS rate.

Within the last decade, the scientific community came to a conclusion that there are several reasons for the lower deposition rates in HPPMS. The major one being metal ion “return effect.” In HPPMS discharges, large fraction of sputtered atoms is ionized due to the dense plasma in front of the target. Some of these newly formed ions return to the target contributing to current increase and cause self-sputtering.¹¹ The sputtered material is ionized close to the target, and the negative potential applied on the target can extend far into

^{a)}Electronic mail: raman6@illinois.edu

the plasma as an extended presheath. In some unbalanced magnetron cases, 10%–20% of the total applied voltage drops in the magnetic presheath, which can extend to 40 mm from the target.¹² Hence, many of the metal ions will be attracted back to the target surface by the cathode potential.¹³ Some of other reasons are yield effect,¹⁴ ion species effect,¹¹ magnetic unbalancing and guiding effect,¹⁵ and an effect in which large fraction of ions of the sputtered material are transported sideways.¹⁶ All named effects are interconnected in HPPMS discharges and have a strong correlation with the plasma parameters. Individual contribution of the effect is hard to quantify and it depends on the magnetic field configuration on the target surface, HPPMS pulsing power supply regime, geometry, etc. For example, Mishra *et al.*¹⁷ reported that with a reduction of magnetic field by 33% at the target surface, the deposition rate of titanium increased by a factor of 6. To summarize, once the HPPMS discharge gets to a state with a high fraction of ionized sputtered material, the electric field distribution inside the plasma prevents ions from escaping the plasma region. The plasma electric potential during the discharge controls the movement of ions, this means the electric potential distribution in plasma during the discharge has to be controlled or at least modified to increase the ion flow away from this trap. There are publications¹⁸ that describe the relationship between magnetic field topology and electric potential distribution inside the plasma. Several attempts to investigate the influence of magnetic field on HPPMS parameters were

done previously and can be summarized as follows: in case of reduced magnetic field strength the ion flux toward the substrate is increased due to the reduction in the metal ions return effect in front of the target.^{19–21}

A forerunner to the work presented here increased the deposition rate by producing a magnetic field, which would allow ions to leave the ionization region and move toward the substrate without being recycled. This idea was tested using a “spiral” magnet pack designed by Yu *et al.*²² This work was continued by shrinking of the 14 in. design to fit into Kurt J. Lesker’s 4 in. TORUS magnetron sputter source. It will be shown in this work that simple scaling will not work, and that further physics existed, and alternative design rules have to be implemented in case of smaller magnetron sputter guns.

II. EXPERIMENTAL SETUP

Sputtering high-purity atomic deposition experiment (SHADE)²³ is a dual magnetron setup for depositing thin films under an ultrahigh vacuum environment. The SHADE chamber [Fig. 1(a)] is equipped with a load lock for sample transfer and a rotatable substrate holder for increasing the uniformity of deposition, the substrate holder can be biased if necessary. A pair of Kurt J. Lesker’s 4 in. TORUS magnetron sputter sources was installed in the SHADE chamber for this work. In this manner, two different magnetic configurations can literally be tested side-by-side keeping all other

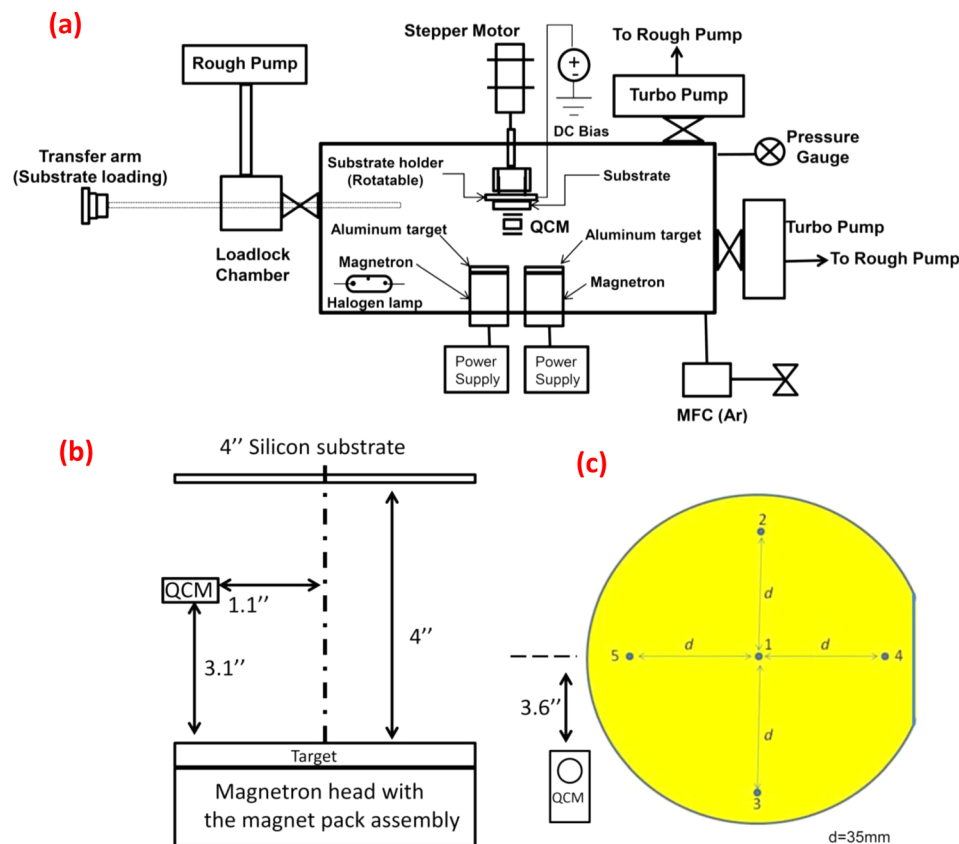


FIG. 1. (Color online) (a) Schematic diagram of the SHADE chamber. (b) Schematic of the 4 in. silicon substrate location with respect to the target. (c) Location of the uniformity test on the 4 in. silicon substrate.

parameters identical. A number of different power supplies were used in this work. An advanced energy pinnacle plus was used for DC and pulsed DC sputtering, for HPPMS, a Huttinger TruPlasma Highpulse 4002 was used (and will be referred to as HiPIMS for high power impulse magnetron sputtering), and a Zpulsor Zpulsor Cyprium VI was used (and will be referred to as MPP for modulated pulse power sputtering). The stainless steel vacuum chamber is pumped by oil free vacuum pumps to a base pressure of 1×10^{-7} Torr. Gas flow into the chamber is controlled by mass flow controllers.

For *in-situ* measurements of deposited film thickness, the SHADE chamber was equipped with an Inficon DLAE47 quartz crystal microbalance (QCM). The location of the QCM is as shown in Figs. 1(b) and 1(c). It was positioned equidistant between the two magnetrons. To increase the accuracy of the QCM, two QCMs (one for control and the other one for actual measurements) were used simultaneously at the same location. Control QCM is masked with a stainless steel shim stock to subtract the noise from thermal drift.

To verify the QCM deposition rate measurement accuracy during HPPMS discharge operation, a half masked test wafer was placed in the actual QCM location. The deposited film thickness on the test wafer was measured using a DEKTA 3030 surface profilometer and it was compared to the QCM thickness readings. The QCM measurement difference between the two techniques was found to be less than 2%. Aluminum targets were used in all the experiments. For the “ ϵ ” magnet pack, which is described later in the paper, a graded-thickness aluminum target was used. The outer rim of the graded aluminum target was 0.125 in. thick and the inner portion was 0.09 in. thick. This design was chosen to sustain a stable HPPMS discharge with the premanufactured magnet set. Slightly stronger magnets in the inner ϵ portion of the epsilon pack would eliminate the need to use a graded target.

III. MAGNET PACK DESIGN AND SIMULATION

In this work, a one-to-one scale 3D model was built in COMSOL Multiphysics finite element analysis software to simulate the magnetic field pattern and electron trajectories above target surface. The “magnetic and electric field”

module of COMSOL Multiphysics was used to calculate the magnetic flux densities and $B_{//} = (\sqrt{B_x^2 + B_y^2})$, XY plane is parallel to the target surface) for any given magnet pack arrangement. The distribution of $B_{//}$ above target allows to predict the racetrack region.¹⁹ Charged particle tracing (CPT) module was used to simulate the electron trajectories above the target surface. Average electron temperatures in HiPIMS discharges are in the order of 0.3–0.4 eV at 20 mTorr.²⁴ In the CPT module, electrons are injected into the race-track on the target surface with energy of 0.1 eV, which is in the range of the average electron energy. This module takes into account electron to electron interaction and particle to field interaction. Total number of particles in a single run is 1000. In every simulation, electrons are released at time step zero and the CPT module resolves particle position at every 0.1 ns. This model for particle tracing is a simplistic way to visualize single particle trajectories and is not intended to directly describe physical phenomena in HPPMS discharge. Scattering and the Hall current are ignored. However, it allows reconstructing a general behavior of electrons in the trap.

A. Conventional magnet pack

A commercially available 4 in. magnetron sputter gun is equipped with a concentric magnet assembly, which gives rise to a circular race track on the target surface. Figure 2(a) shows the shape and magnitude of $B_{//}$ field on the XY plane of the target surface. X and Y axes represent the physical dimension in inches of the target. Figure 2(b) shows the streamline plot of magnetic field lines in XZ plane, B_x and B_z (magnetic field component along x and z directions) of the conventional magnet pack.

At time $t = 0$, electrons start to gyrate along the magnetic field and drift in the $E \times B$ direction as shown in Figs. 3(a). Figure 3(b) shows the full electron trajectory in $E \times B$ direction at $1 \mu s$. It can be seen from Fig. 3(c) that the electrons are trapped efficiently above the target surface and are recycled. This process is well described by Anders *et al.*²⁵ and various books. The different colors in the electron trajectory plots represent the electron velocities. While their values are not relevant for this work, maximum is 3.5×10^6 m/s going to minimum at 0.5×10^6 m/s. One can see that in the conventional magnet pack, the electron trap is highly

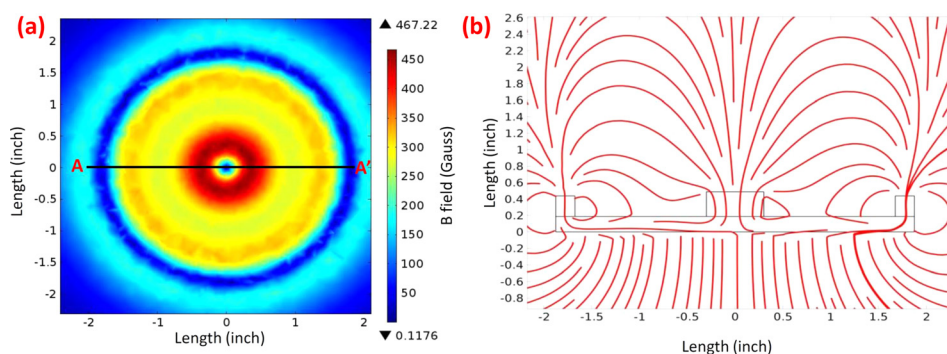


FIG. 2. (Color online) (a) $B_{//}$ on the target surface of the conventional magnet pack, line AA' shows the location of the cut section. (b) Streamline plot of B_x and B_z components in the XZ plane cut section along AA', the field lines represents the B_x and B_z components.

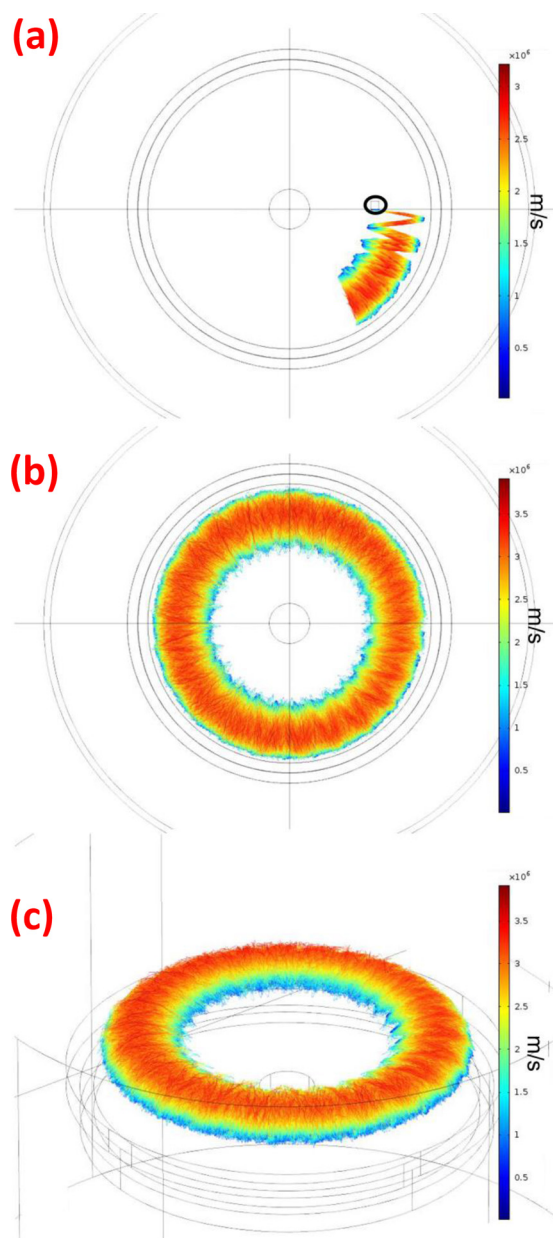


FIG. 3. (Color online) Electron trajectory of the conventional magnet pack at times (a) $t = 100$ ns, (b) $t = 1000$ ns, (c) electron trajectory at time $t = 1000$ ns in a 3D view. Electrons are started with 0.1 eV in the middle of the race track at the 3 o'clock position as indicated by the black circle in Fig. 3(a).

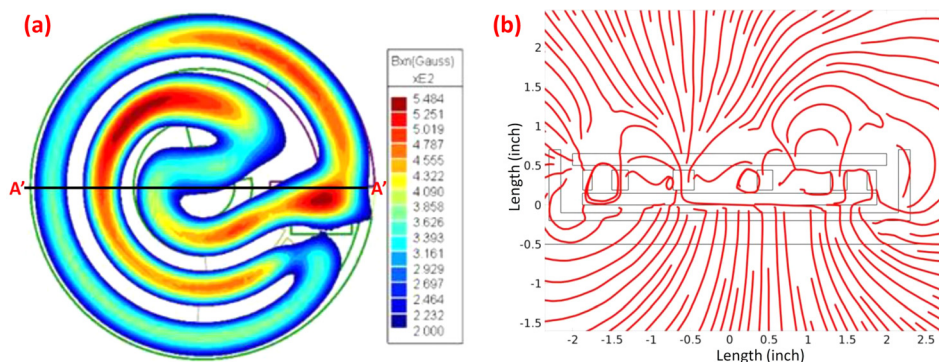


FIG. 4. (Color online) (a) B_{\parallel} on the target surface of the spiral magnet pack, line AA' shows the location of the cut section. (b) Streamline plot of B_x and B_z components in the XZ plane cut section along AA', the field lines represents the B_x and B_z components. The DC I-V plot of 4 in. spiral magnet pack at 40 mTorr is shown in Fig. 8 along with I-V curves for conventional and ϵ magnet packs.

efficient, which in turn makes the HPPMS ion recycling process also very efficient.

B. Spiral magnet pack

The 4 in. spiral magnet pack is the scaled down version of the 14 in. spiral pack described by Yu *et al.*²² The magnet pack assembly was manufactured by Dexter Magnetic Technologies, Inc. Figure 4(a) is the simulated B_{\parallel} of the 4 in. spiral design, and Fig. 4(b) is the streamline plot of B_x and B_z components.

Experiments on the spiral magnet pack showed that the discharge current density of this magnet pack saturates at about 18 mA/cm^2 as shown in Fig. 8. The discharge does not get in to the high current mode even at voltages above 1500 V and also the discharge cannot be ignited at pressures lower than 40 mTorr. It is clear that the spiral pack is not operating in the magnetron mode²⁶ when scaled down to a smaller size, and also the HPPMS high current mode cannot be achieved. The reason for this current limit is electron leak from racetrack.

It can be observed from Fig. 4(b) that the magnetic field lines near the target surface are open, unlike in a conventional magnet pack. It can be seen from Figs. 5(b) and 5(c) that the sharp magnetic field gradients (greater than 50 G/cm) and low magnetic field regions (below 200 G) lead to a situation, where no more than 5% of all electrons are efficiently recycled inside the race-track.

Although the spiral design on the 14 in. magnet pack gave a high discharge current as discussed by Yu *et al.*,²² this design does not work for the 4 in. sputter guns. A possible explanation behind the working of the 14 in. spiral pack is that the length of the 14 in. target racetrack is long enough such that a secondary electron has at least one collision with neutrals before it leaks out of the racetrack. This is not true in the 4 in. design. Furthermore, the importance of the potential distribution, and balance between ion leakage and electron trapping was not anticipated in Yu *et al.*²² Higher gradients in the field along the pack, and higher radii of curvature at the bends also provide more leakage opportunities.

To summarize, the magnetic field simulation and experimental results from the direct scaling of 14 in. spiral pack down to 4 in. provide several design guidelines:

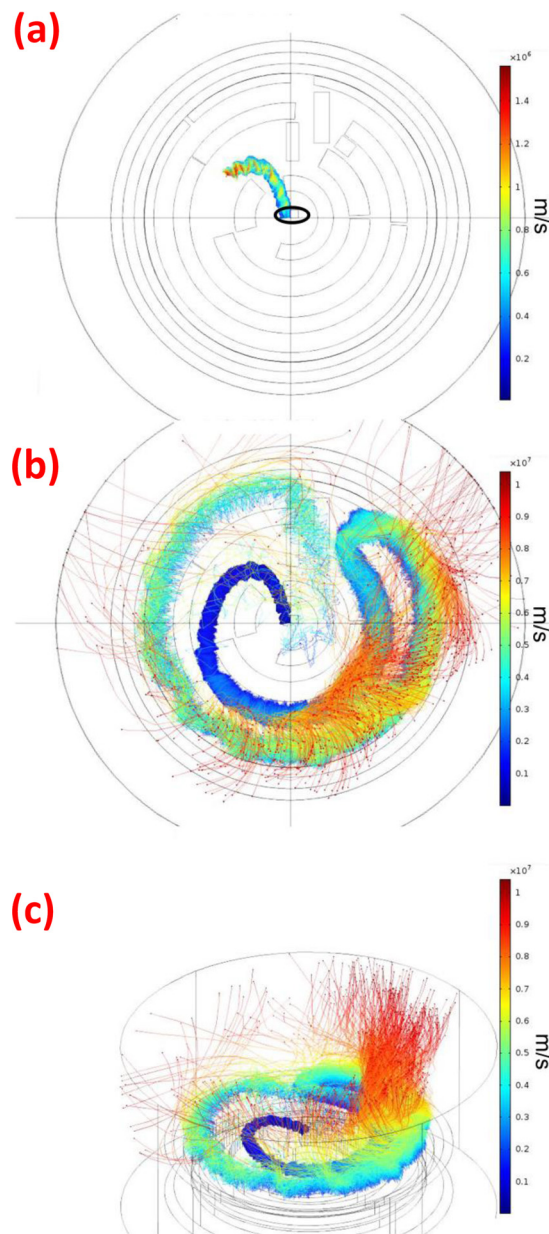


FIG. 5. (Color online) (a) Electron trajectory of the spiral magnet pack at times (a) $t = 100$ ns, (b) $t = 1000$ ns, and (c) electron trajectory at time $t = 1000$ ns in a 3D view. Electrons are started with 0.1 eV in the middle of the race track at the position indicated by the black circle in Fig. 5(a).

- (1) Sharp turn on the electrons path will cause intense leakage. Recent studies show that high density plasma spikes^{27,28} that are observed in HPPMS discharges might not be able to make it through a turn radius of more than 4 mm.
- (2) The various magnet pack designs simulated in COMSOL show that gradients of magnetic field along race track path should not be steeper than 50 G/cm to ensure sufficient electron confinement.

In order to overcome these problems and follow these guidelines, a new ϵ design was developed.

C. ϵ magnet pack

The surface magnetic field above target in the ϵ magnet pack configuration is shown in Fig. 6(a), and Fig. 6(b) shows

the B_x and B_z components in the XZ plane cut section along AA'. The racetrack consists of an outer circular area with a uniform magnetic field and an inner “Epsilon” shaped area with lower magnetic flux density, less sharp $B_{||}$ gradients than the spiral pack but similar sharp turns as in the spiral design. The magnetic field on the outer racetrack is about 400 G and the inner race track is between 275 and 350 G. The outer racetrack provides stable ignition at lower pressures and constant electron feed into the inner racetrack. The inner racetrack has a specially designed magnetic field line profile, which sustains an electron leakage from the central portion. The lower $B_{||}$ in the inner race track and open field lines provide higher ion flux along the axis of the magnetron in the direction away from the target. Although ϵ has a region of electron leakage, it can achieve a sustainable high current pulsed discharge regime and setup a potential distribution, which allows more ions to escape in comparison to the conventional magnet pack. Note that the fields in the conventional magnet pack are very similar in magnitude. The highest values are 400 G and over the bulk of the race track, the values are 275–350 G. The difference in performance is not due to merely lowering the magnetic field magnitudes.

Confinement and electron loss paths of this magnet pack can be observed in Figs. 7(b) and 7(c). This pack sustains discharges with volt-ampere characteristics that follow a well-known magnetron mode $I \propto V^n$ relationship, where “n” is the performance index of the electron trap²⁶ as shown in Fig. 8.

Figure 8 is the plot of discharge voltage versus current density. Current density here represents the ratio of the peak discharge current by the total race track area specific to the magnet pack. Conventional pack and ϵ pack follow the magnetron mode, whereas the 4 in. spiral pack does not allow this mode.

In Fig. 9, solid legends represent conventional pack and hollow legends represent ϵ pack. It can be seen that the ϵ pack Huttinger HiPIMS power supply gives higher deposition rates than MPP Zpulsar power supply and also it gives twice higher deposition rates than conventional pack HiPIMS discharges for the same average power. In all these experiments, Huttinger HiPIMS power supply was operated at 200 Hz, 1.5% duty cycle, Zpulsar MPP supply was operated at 100 Hz, 10% duty cycle, and AE pulsed DC power supply was operated at 5 kHz and 97.5% duty cycle. Due to asymmetry of the “ ϵ ” magnet pack, the deposition rates were measured for different orientations of the pack. This was done by rotating the magnetron gun every 90° along the central axis and recording the deposition rates from the QCM. The deposition rates from the four different orientations were found to be the same, within 1% or less. Deposition rates beyond 500 W are not presented for the conventional pack with Huttinger HiPIMS power supply due to the melting of the target. It can also be seen from Fig. 9, that the ϵ pack Huttinger HiPIMS deposition rates at the off-center position reaches to almost 80% of conventional DC sputtering at an average power of 400 W.

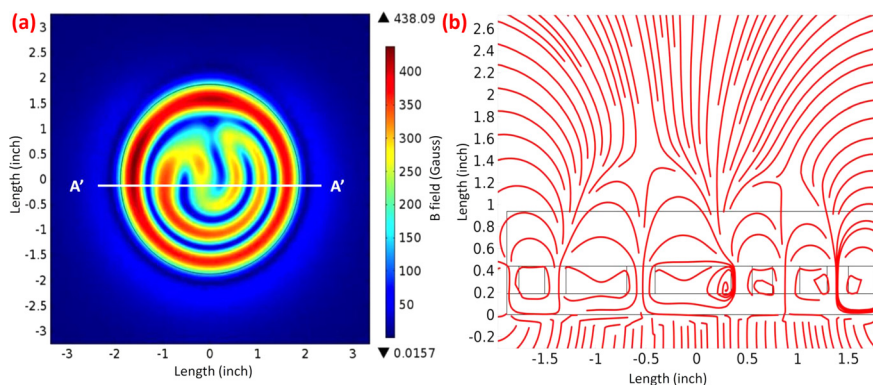


FIG. 6. (Color online) (a) B_{\parallel} on the target surface of the ϵ magnet pack, line AA' shows the location of the cut section. (b) Streamline plot of B_x and B_z components in the XZ plane cut section along AA', the field lines represents the B_x and B_z components.

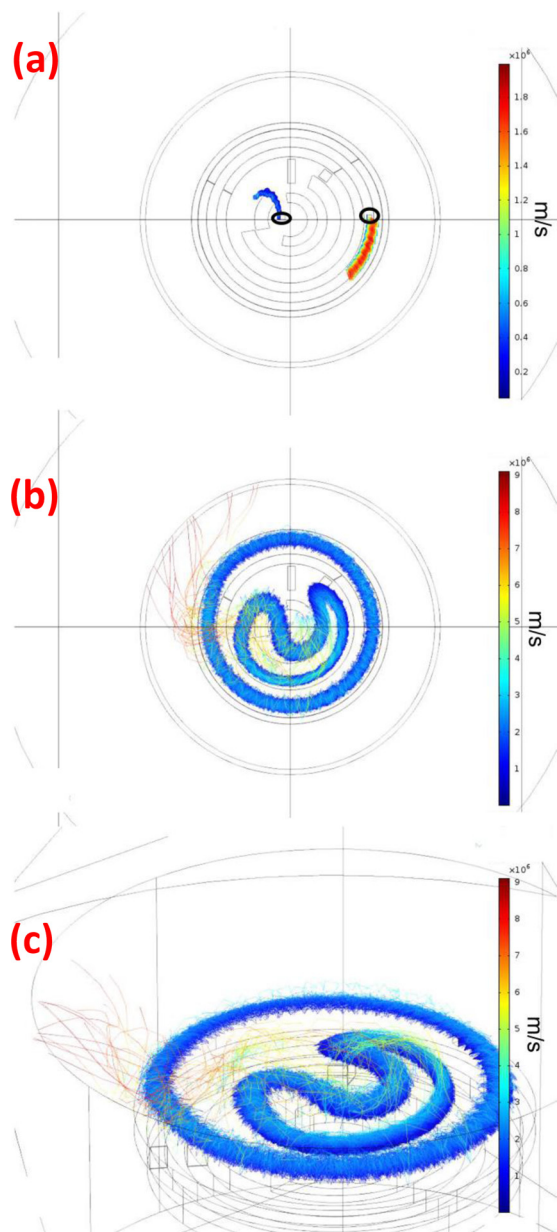


FIG. 7. (Color online) (a) Electron trajectory of the ϵ magnet pack at times (a) $t = 100$ ns, (b) $t = 1000$ ns, and (c) electron trajectory at time $t = 1000$ ns in a 3D view. Electrons are started with 0.1 eV in the middle of the race track at positions indicated by the black circle in Fig. 6(a).

In order to test the uniformity of deposition, 4 in. silicon wafers were placed 4 in. coaxially away from the target as shown in Fig. 1(b). The thickness of the deposited films was measured using x-ray reflectivity (XRR) technique. A PANalytical MRD X'pert x-ray diffraction system was used for this purpose. The deposited film thickness was measured for ϵ pack Huttinger HiPIMS, conventional pack HiPIMS and conventional pack DC at 10 mTorr and 500 W average power at the locations shown in Fig. 1(c). The overall uniformity of the ϵ pack was similar to that of the conventional pack, which can be observed from Table I. Table I shows the deposition rates measured using XRR technique at five different locations on the 4 in. wafer as shown in Fig. 1(c). Table II is the average deposition rates from ϵ and conventional magnet pack for Huttinger HiPIMS and DC power supplies at 10 mTorr and 500 W average power from different locations on the 4 in. wafer during uniformity experiments. It can be observed from Table II that the average deposition rates for all positions with ϵ pack Huttinger HiPIMS was $8.8 \pm 0.4 \text{ \AA/s}$, with conventional pack HiPIMS was $4.1 \pm 0.2 \text{ \AA/s}$ and with conventional pack DC was $12.1 \pm 0.6 \text{ \AA/s}$. The ϵ pack Huttinger HiPIMS gives about twice higher deposition rate than conventional pack with HiPIMS discharges even when the substrate is placed line of

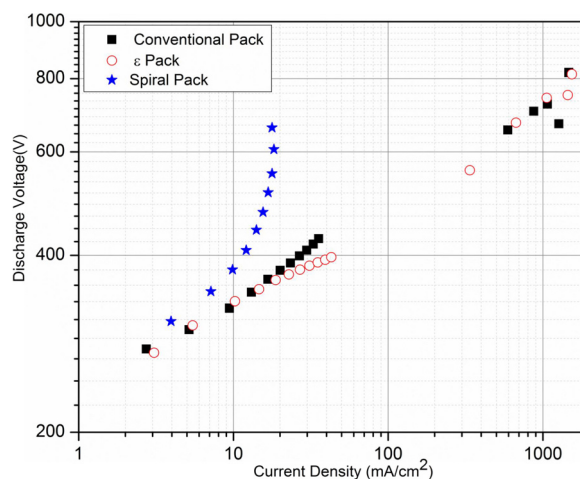


FIG. 8. (Color online) IV characteristic of conventional, ϵ magnet pack at 10 mTorr and spiral pack at 40 mTorr.

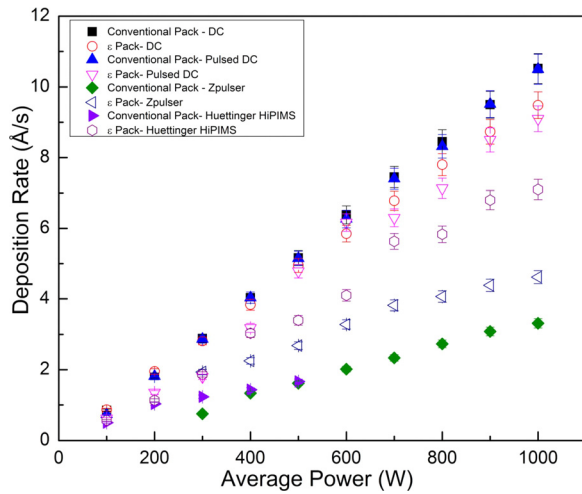


FIG. 9. (Color online) Summary of QCM deposition rates for both the magnet packs with different power supplies at 10 mTorr measured at the QCM.

sight to the target. These data points agree well with the data obtained by QCM earlier.

The total racetrack length for the conventional pack is 9.35 and 18.7 in. is for the ϵ pack [Fig. 10(c)]. However, this difference in race track length does not explain the higher deposition of the ϵ pack. The total erosion area for the conventional pack is 10.2 and 9.1 in.² for the ϵ pack since the conventional pack has a very broad erosion groove. The peak current at an average power of 500 W with the conventional pack was ~ 95 and ~ 78 A with the ϵ pack. Therefore, the current density was 1400 mA/cm² for the conventional pack and 1300 mA/cm² for the ϵ pack. These values are very close. Since the current density and currents are similar, the reason for the significantly higher deposition rate must be due to confinement and return of sputtered material, not the generation of sputtered material.

Since the race track area was approximately the same for both magnet packs, one would expect the similar peak currents, but it can be observed from Figs. 11(a) to 11(d) that in the case of ϵ pack, the peak current is lower than that of the conventional pack with Huettinger HiPIMS and Zpulsar MPP supplies. These IV Oscillogram trends clearly points to plasma mechanics behind deposition rate increase. Peak currents are lower because not all of the ionized metal atoms are recycled back to the target. It can be observed from Figs.

TABLE I. Deposition rates from ϵ and conventional magnet pack for Huettinger HiPIMS and DC power supplies at 10 mTorr and 500 W average power at locations indicated in Fig. 1(c) during wafer uniformity experiments.

| Position | DC deposition rates (Å/s) | | HiPIMS deposition rates (Å/s) | |
|----------|---------------------------|------------|-------------------------------|---------------|
| | Conventional | ϵ | Conventional | ϵ |
| 1 | 12.5 \pm 0.6 | — | 4.2 \pm 0.2 | 9.6 \pm 0.5 |
| 2 | 12.3 \pm 0.6 | — | 4.2 \pm 0.2 | 8.4 \pm 0.4 |
| 3 | 11.6 \pm 0.6 | — | 3.8 \pm 0.2 | 8.4 \pm 0.4 |
| 4 | — | — | — | 9.1 \pm 0.5 |
| 5 | — | — | — | 8.6 \pm 0.4 |

TABLE II. Average deposition rates from ϵ and conventional magnet pack for Huettinger HiPIMS and DC power supplies at 10 mTorr and 500 W average power during wafer uniformity experiments.

| Magnet pack | DC deposition rate (Å/s) | HiPIMS deposition rate (Å/s) |
|--------------|--------------------------|------------------------------|
| Conventional | 12.1 \pm 0.5 | 4.1 \pm 0.2 |
| ϵ | — | 8.8 \pm 0.5 |

11(c) and 11(d) that Zpulsar MPP generates 1 ms long pulse (macropulse) that is composed of a train of 20–30 μ s long micropulses.

The deposited aluminum films were characterized using Hitachi S-4800 scanning electron microscope (SEM). Films grown using ϵ magnet pack with Huettinger HiPIMS power supply under the same conditions as conventional pack show much smaller grain structure and can be observed from Figs. 12(b) and 12(c).

Here, we would like to summarize some experimental observations to discuss the reason for twice higher deposition rate in HPPMS with ϵ magnetic configuration:

- (1) $B_{||}$ in the middle of the race track for conventional and ϵ magnet packs are nearly identical. It is about 400–300 G for ϵ and about 300 G for the conventional pack.
- (2) The peak current in the ϵ pack is only 10% lower than the peak current in the conventional pack during a single HPPMS discharge.
- (3) The IV Oscillograms traces do not show any anomalous differences in the case of Huettinger HiPIMS power supply [Figs. 11(a) and 11(b)]. But a different trend is observed in Zpulsar power supply, which is seen Figs. 11(c) and 11(d).



FIG. 10. (Color online) (a) Graded 4 in. Al target. (b) Race track erosion pattern on the 4 in. Al target from conventional magnet pack. (c) Race track erosion pattern on the 4 in. Al target from spiral magnet pack. (d) Race track erosion pattern on the 4 in. Al target from ϵ pack.

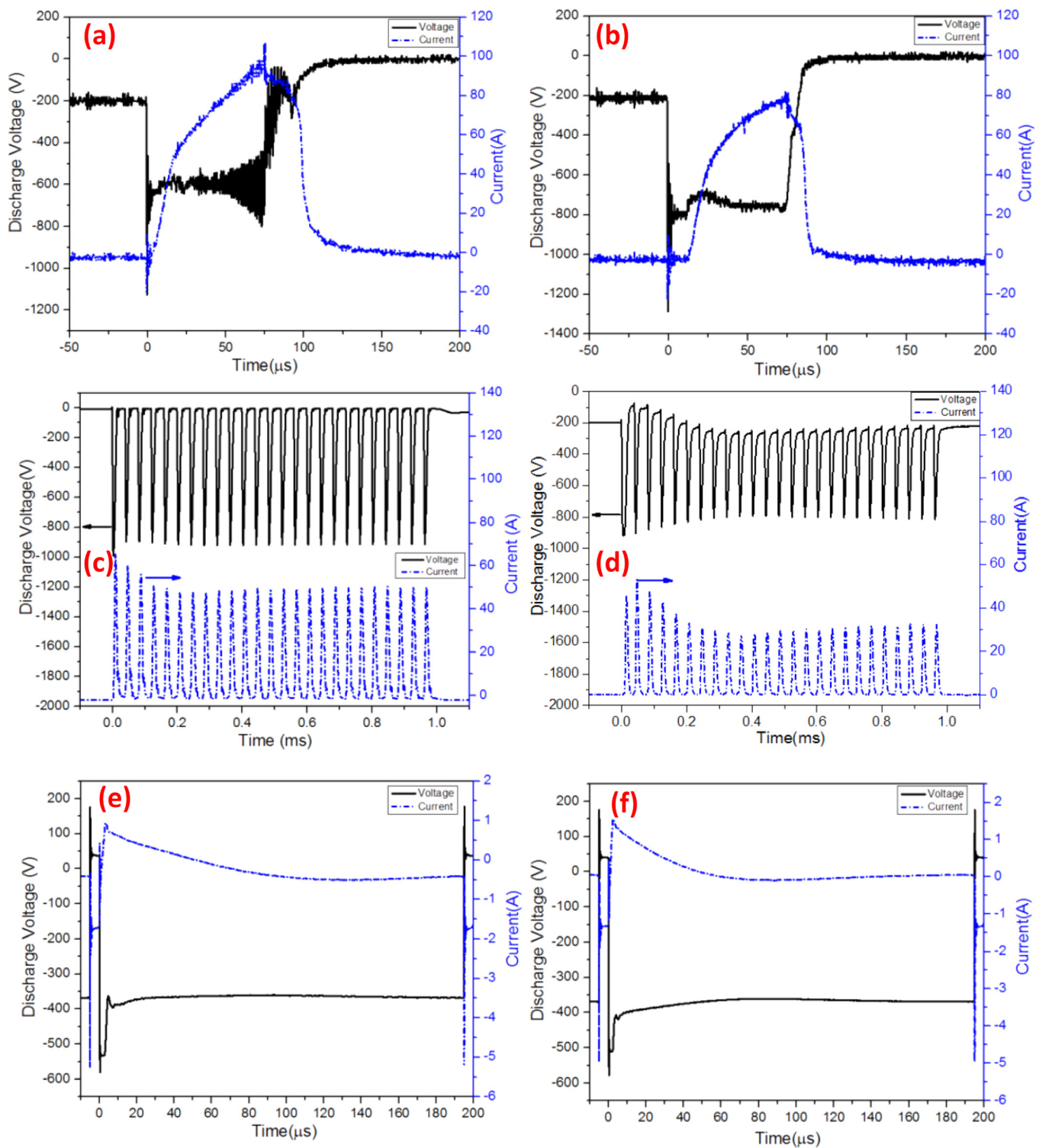


FIG. 11. (Color online) VI oscillograms from (a) conventional pack Huttinger HiPIMS power supply, (b) ϵ pack Huttinger HiPIMS power supply, (c) conventional pack Zpulsar MPP supply, (d) ϵ pack Zpulsar MPP supply, (e) conventional pack AE pulsed DC power supply, and (f) ϵ pack AE pulsed DC power supply.

(4) The film microstructure with Huttinger HiPIMS power supply is very different for ϵ and conventional pack. Films grown using ϵ magnet pack under the same conditions as conventional pack (pressure and gas) show much smaller grain structure, which can be observed from Figs. 12(b) and 12(c).

These experimental observations point to the measured increase in deposition rate being due to differences in the plasma transport properties of ϵ and conventional magnetic field configurations. Since the race track area was approximately the same for both magnet packs, one would expect the similar peak currents, but it can be observed from

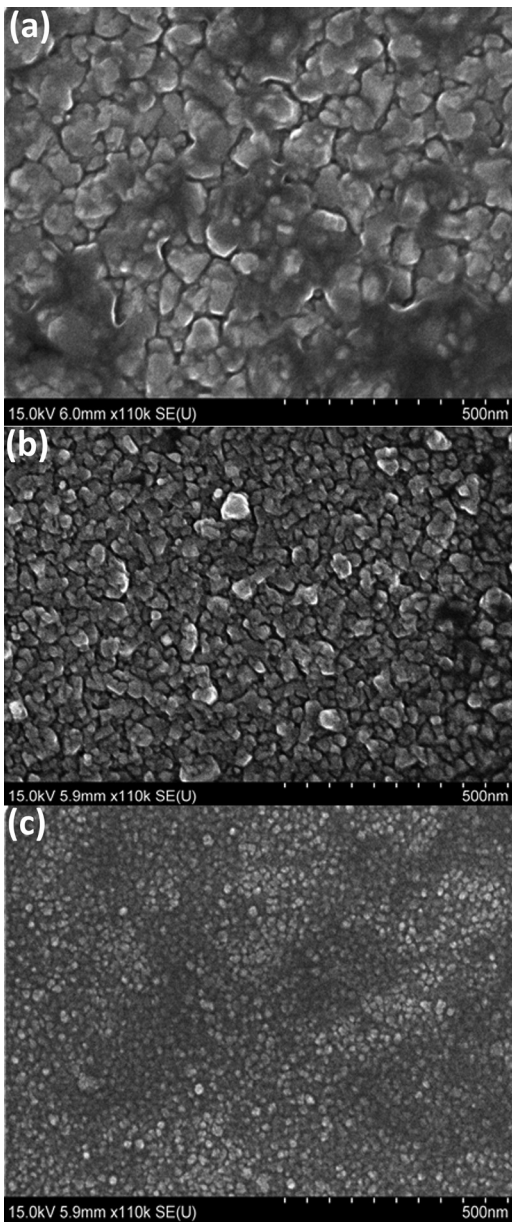


FIG. 12. (a) SEM image of conventional pack aluminum film deposited using DC power supply. (b) SEM image of conventional pack aluminum film deposited using Huttinger HiPIMS power supply. (c) SEM Image of ϵ pack aluminum film deposited using Huttinger HiPIMS power supply.

Figs. 11(a) to 11(d) that in the case of ϵ pack, the peak current is lower than that of the conventional pack although the voltage is slightly higher. This means approximately the same amount of sputtered material is supplied to the plasma region in case of ϵ pack. However, fewer ions are returned to the target. The difference between the Huttinger HiPIMS results and the Zpulsar MPP results are consistent with the following observation. There is a change in slope at $20\ \mu\text{s}$ in Figs. 12(a) and 12(b). It is believed that this is the point where metal self sputtering becomes dominant and the HPPMS mode is realized.²⁹ At this point, the current is 50 A, but then rises to nearly 100 A. Each of the independent MPP pulses lasts only $20\text{--}25\ \mu\text{s}$ and follows the same initial slope and shape as the first $20\ \mu\text{s}$ of the HiPIMS pulse. Indeed,

they only reach 50 A. Since the peak current is not as high in the MPP discharges as it is in the HiPIMS discharges, not as much material is sputtered. This can explain the lower deposition rates for MPP. Since similar amounts of material are supplied to the plasma region but more material is delivered to the substrate, it must be the case that more material is transported across the field toward the substrate. The efficiency of the ionized Al trap is poorer. The difference in the microstructure of the films grown using ϵ pack and conventional pack [Figs. 12(b) and 12(c)] clearly indicates that the deposition flux consisted of more ions, though it is not a solid proof, this is the most probable explanation. Based on the assumption that the material flux consist more of ions, then even in conventional pack HPPMS discharge, we can assume that more ions escape from the plasma region. This higher ion flux has to be compensated by electrons following ions otherwise trapped by magnetic field electrons would suppress flux dramatically. The higher electron flux can be only due to magnetic field topology, which implements “opened field lines” allowing electrons to escape plasma region. On the other hand, the trap has much sharper magnetic field gradients along “z” direction, which also may impact the increased ion flux toward the substrate.

This proposed explanation needs to be verified via direct measurements of ion flux toward the substrate and will be in the future work, but the experimental observations are all consistent with this explanation.

IV. SUMMARY AND CONCLUSIONS

A magnetic field design, which obtains higher deposition rates and higher target utilization than conventional magnetic field designs in HPPMS discharge, has been developed.³⁰ It was shown that the correct selection of magnetic field strength and configuration is critical to achieve a sustainable high-current pulsed-discharge mode. Scaling magnetic packs proportionally does not necessarily work for all designs. An understanding of the effect of the magnet field and potential distribution in the plasma is critical. The proposed ϵ magnet pack combines advantages of conventional magnetron magnet pack discharge stability with the higher ion fraction and better film characteristics of a HPPMS discharge. It also has an increased deposition rate with full-face target erosion compared to conventional systems. It differs from an unbalanced magnetron configuration in that there is intentional confinement of the electrons, but at a larger distance from the surface of the target, where the electric field in the presheath should be smaller.

ACKNOWLEDGMENTS

This research was funded by NSF Center for Lasers and Plasmas for Advanced Manufacturing under I/UCRC program. This work was carried out in part in the Frederick Seitz Materials Research Laboratory Central Research Facilities and Visualization laboratory at Beckman Institute in University of Illinois. The authors would like to thank Mauro Sardela for his help with XRR measurements.

- ¹P. Kelly and R. Arnell, *Vacuum* **56**, 159 (2000).
- ²J. A. Hopwood, *Thin Films* **27**, 1 (2000).
- ³U. Helmersson, M. Lattemann, J. Bohlmark, A. P. Ehiasarian, and J. T. Gudmundsson, *Thin Solid Films* **513**, 1 (2006).
- ⁴J. Alami, J. T. Gudmundsson, J. Bohlmark, J. Birch, and U. Helmersson, *Plasma Sources Sci. Technol.* **14**, 525 (2005).
- ⁵J. Alami, S. Bolz, and K. Sarakinos, *J. Alloys Compd.* **483**, 530 (2009).
- ⁶V. Kouznetsov, K. Macák, J. M. Schneider, U. Helmersson, and I. Petrov, *Surf. Coat. Technol.* **122**, 290 (1999).
- ⁷A. Anders, *Appl. Phys. Lett.* **92**, 201501 (2008).
- ⁸J. Alami, K. Sarakinos, G. Mark, and M. Wuttig, *Appl. Phys. Lett.* **89**, 154104 (2006).
- ⁹D. Mozgrin, I. Fetisov, and G. Khodachenko, *Plasma Phys. Rep.* **21**, 400 (1995).
- ¹⁰M. Samuelsson, D. Lundin, J. Jensen, M. A. Raadu, J. T. Gudmundsson, and U. Helmersson, *Surf. Coat. Technol.* **205**, 591 (2010).
- ¹¹A. Anders, *J. Vac. Sci. Technol., A* **28**, 783 (2010).
- ¹²A. Rauch, R. J. Mendelsberg, J. M. Sanders, and A. Anders, *J. Appl. Phys.* **111**, 083302 (2012).
- ¹³D. Christie, *J. Vac. Sci. Technol. A* **23**, 330 (2005).
- ¹⁴J. Emmerlich, S. Mráz, R. Snyders, K. Jiang, and J. M. Schneider, *Vacuum* **82**, 867 (2008).
- ¹⁵J. Bohlmark, M. Östbye, M. Lattemann, H. Ljungcrantz, T. Rosell, and U. Helmersson, *Thin Solid Films* **515**, 1928 (2006).
- ¹⁶D. Lundin, P. Larsson, E. Wallin, M. Lattemann, N. Brenning, and U. Helmersson, *Plasma Sources Sci. Technol.* **17**, 035021 (2008).
- ¹⁷A. Mishra, P. Kelly, and J. Bradley, *Plasma Sources Sci. Technol.* **19**, 045014 (2010).
- ¹⁸B. Liebig and J. Bradley, *Plasma Sources Sci. Technol.* **22**, 045020 (2013).
- ¹⁹A. P. Ehiasarian, *Proceedings of the 52nd Annual Conference Society of Vacuum Coaters*, Santa Clara, CA (2009).
- ²⁰L. Meng, H. Yu, M. M. Szott, J. T. McLain, and D. N. Ruzic, *J. Appl. Phys.* **115**, 223301 (2014).
- ²¹J. Capek, M. Hála, O. Zabeida, J. E. Klemberg-Sapieha, and L. Martinu, *J. Phys. D: Appl. Phys.* **46**, 205205 (2013).
- ²²H. Yu, L. Meng, M. M. Szott, J. T. McLain, T. S. Cho, and D. N. Ruzic, *Plasma Sources Sci. Technol.* **22**, 045012 (2013).
- ²³E. Ritz, Y. L. Wu, J. Hong, D. Andruczyk, T. S. Cho, and D. N. Ruzic, *Surf. Coat. Technol.* **251**, 64 (2014).
- ²⁴J. T. Gudmundsson, P. Sigurjonsson, P. Larsson, D. Lundin, and U. Helmersson, *J. Appl. Phys.* **105**, 123302 (2009).
- ²⁵A. Anders, J. Andersson, D. Horwat, and A. Ehiasarian, *The Ninth International Symposium on Sputtering and Plasma Processes (ISSP)* (2007).
- ²⁶J. A. Thornton, *J. Vac. Sci. Technol.* **15**, 171 (1978).
- ²⁷A. Anders, P. Ni, and A. Rauch, *J. Appl. Phys.* **111**, 053304 (2012).
- ²⁸N. Brenning, D. Lundin, T. Minea, C. Costin, and C. Vitelaru, *J. Phys. D: Appl. Phys.* **46**, 084005 (2013).
- ²⁹L. Meng, "Comparison of high power impulse magnetron sputtering and modulated pulsed power sputtering for interconnect metallization," Ph.D. dissertation (University of Illinois at Urbana-Champaign, 2013).
- ³⁰D. N. Ruzic, P. Raman, and I. Shchelkanov, U.S. patent, provisional patent application, 62/076,931 (7 November 2014).